

AD-A267 559



Computer Science

DTIC  
S ELECTE D  
AUG 5 1993  
C

Computing the Pipelined Phase-Rotation FFT

Langhorne P. Withers, Jr., John E. Whelchel,  
David R. O'Hallaron, Peter J. Lieu

July 13, 1993  
CMU-CS-93-174

DTIC QUALITY

DISTRIBUTION STATEMENT A

Approved for public release  
Distribution Unlimited

Carnegie  
Mellon

93-17731



1995

## Computing the Pipelined Phase-Rotation FFT

Langhorne P. Withers, Jr., John E. Welchel,  
David R. O'Hallaron, Peter J. Lieu

July 13, 1993  
CMU-CS-93-174

DTIC QUALITY INSPECTED 3

School of Computer Science  
Carnegie Mellon University  
Pittsburgh, PA 15213

David O'Hallaron and Peter Lieu are in the School of Computer Science at Carnegie Mellon. Lang Withers and John Welchel are with E-Systems, Inc..

### Abstract

The phase-rotation FFT is a new form of the FFT that replaces data movement with multiplications by constant phasor multipliers. The result is an FFT that is simple to pipeline. This paper reports some fundamental new improvements to the original phase-rotation FFT design, provides a complete description of the algorithm directly in terms of the parallel pipeline, and describes a radix-2 implementation on the iWarp computer system that balances computation and communication to run at the full-bandwidth of the communications links, regardless of the input data set size.

Supported in part by the Advanced Research Projects Agency, Information Science and Technology Office, under the title "Research on Parallel Computing," ARPA Order No. 7330. Work furnished in connection with this research is provided under prime contract MDA972-90-C-0035 issued by ARPA/CMO to Carnegie Mellon University, and in part by the Air Force Office of Scientific Research under Contract F49620-92-J-0131. Also supported in part by an E-Systems IR&D program

Accession For	
NTIS CRA&I	<input checked="" type="checkbox"/>
DTIC TAB	<input type="checkbox"/>
Unannounced	<input type="checkbox"/>
Justification	
By	
Distribution /	
Availability Codes	
Dist	Avail and/or Special
A-1	

**Keywords:** multicomputers, signal processing, Fast Fourier Transform

## 1. Introduction

The Fast Fourier Transform (FFT) is an important algorithm with many applications in signal processing and scientific computing. The Whelchel phase-rotation FFT [9] derives from the Pease constant-geometry FFT [7], which itself derives from the original Cooley-Tukey FFT [4] expressed in terms of Kronecker products.

The phase-rotation FFT of radix  $r$  is designed for a pipeline of  $r$  parallel data channels. At each time step, in each stage, the pipeline carries the next  $r$  data points, one from each channel, into a Discrete Fourier Transform (DFT) kernel. Unlike earlier pipelined FFT's [5, 6], the phase-rotation FFT has the key property that no data is switched across channels, except within the DFT kernel and at the input and output. The phase-rotation approach extends easily to higher radices, reducing memory and latency while preserving the high throughput and parallel shuffling simplicity of lower radix versions. The phase-rotation FFT has also been extended to a vector-radix, multidimensional parallel-pipeline FFT with the same qualities of the one-dimensional algorithm, and without transposes [10].

This paper describes the results of a project to implement the phase-rotation FFT on a parallel computer system. There are three main results: First, the digit-reversing shuffle step in the original version of the phase-rotation FFT [9] is a potential pipeline bottleneck because it requires communication between the data channels. We describe a new version that corrects this problem by using a parallel-pipeline digit-reversing step.

Second, although the structure of the phase-rotation FFT is extremely simple, we have learned from experience that generating the appropriate twiddles and shuffle indices from the original matrix formulation [9] is quite difficult, even for the designers of the algorithm! To try to help the implementer, we have reformulated the phase-rotation FFT. We present a new set of recipes for generating the twiddles and shuffle indices directly in terms of the parallel pipeline.

Finally, we describe mapping strategies for the phase-rotation FFT on the iWarp, a parallel computer system developed by Intel and Carnegie Mellon [1, 2]. We describe a *fine-grained approach* for an  $N$ -point radix-2 phase-rotation FFT that balances computation and communication to run at the full 40 Mbytes/sec rate of the iWarp physical links, regardless of the size of the input data sets.

Section 2 introduces the phase-rotation concept. Section 3 formally defines the improved FFT algorithm. Section 4 gives the recipes for generating the twiddles and shuffle indices in terms of the parallel pipeline. Finally, Section 5 describes the full-bandwidth implementation on iWarp.

## 2. The basic idea

This section introduces the concept of the phase-rotation FFT. Starting with the Pease constant-geometry FFT, we informally derive the pipelined phase-rotation FFT, identifying the key insights along the way.

## 2.1. Constant-geometry FFT

Figure 1(a) shows the flowgraph for a radix- $r$   $N$ -point decimation-in-frequency (DIF) constant-geometry FFT, with  $r = 2$  and  $N = r^n = 8$ . There are  $n$  stages. Each stage contains  $N/r$  kernels. Each kernel is an operator that performs an  $r$ -point DFT. For radix 2, each kernel inputs two complex numbers and outputs two complex numbers. (For simplicity, twiddles are not explicitly shown in the flowgraph.)

Each stage in the constant-geometry FFT performs an identical perfect stride-by- $s$  shuffle of its data vector, where  $s = N/r$ . If the data vector is regarded as an  $s \times r$  array, stored in column-major order, then the perfect shuffle simply transposes it into an  $r \times s$  array. For example, the following transpose is a stride-by-4 perfect shuffle, for  $N = 8$  points and radix  $r = 2$ :

$$\begin{bmatrix} 0 & 4 \\ 1 & 5 \\ 2 & 6 \\ 3 & 7 \end{bmatrix} \xrightarrow{T} \begin{bmatrix} 0 & 1 & 2 & 3 \\ 4 & 5 & 6 & 7 \end{bmatrix}$$

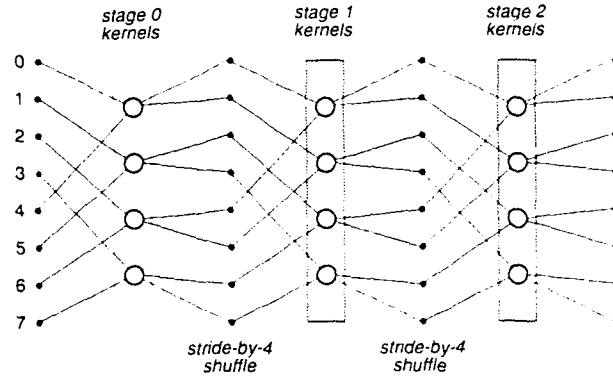
The data items in example above, labeled by their indices in the original column vector, are regarded as equivalent to a  $4 \times 2$  array composed by a stride-by-4 unstacking of the 8-point column vector. After the transpose, the  $2 \times 4$  array is equivalent to a new 8-point column vector composed by a stride-by-2 stacking. As we shall see, this transpose creates difficulties when we try to pipeline the constant-geometry FFT. And it is precisely these difficulties that the phase-rotation FFT addresses.

## 2.2. Pipelining the FFT

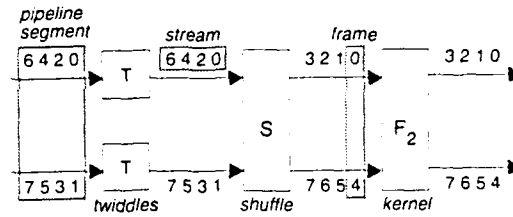
Each stage of the constant-geometry FFT can be computed on a single processor by pipelining the data. For example, Figure 1(b) shows the pipeline for a single stage with radix  $r = 2$ . The pipeline consists of a sequence of operators connected by *pipeline segments*. Each pipeline segment consists of  $r$  parallel *channels*. Each channel carries a *stream* of  $N/r$  data points, which are labeled in this example by their indices from the original column vectors in Figure 1(a). For each pipeline segment, the  $r$  data points in the same position in each stream are known as an  $r$ -*frame*, or simply, a *frame*. For example, in Figure 1(b), the first frame in the pipeline segment between S and F is (0,4), the second frame is (1,5), and so on.

At each time step, the  $r$  twiddle operators (T) collectively read a frame (one complex number per operator), perform an element-wise complex multiplication, and write the resulting frame. Notice that each stream is operated on independently. Similarly, the kernel operator (F) reads a frame, computes the radix- $r$  kernel, and writes the resulting frame. In this case, the streams are not independent; each data item in the output frame is a function of every data point in the input frame.

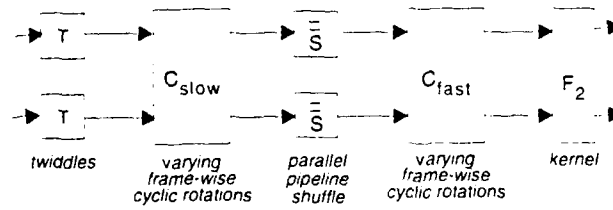
The twiddle and kernel operators pipeline nicely because during each time step they independently read and write a single number. However, the pipelined shuffle operator (S) is less well behaved. To produce one output frame, the shuffle operator must read and store the  $r$  data points from each stream. Thus, S requires  $r$  memory cycles to produce each frame. (Notice that S transposes the data directly into an  $r \times s$  pipeline segment; even starting with data already in an  $r \times s$  pipeline, S still performs "row-to-column" motions.) This is an example of the *memory-bank conflict* discussed in [8, pp.31-32]. The conflict is clear in Figure 1(b). To assemble its first output frame, S must read both 0 and 4 from the upper stream to its left. Then it must read 1 and 5 from the lower stream, and so on.



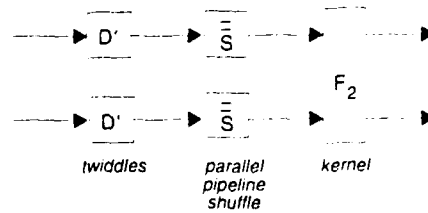
(a)



(b)



(c)



(d)

**Figure 1: Derivation of the phase-rotation FFT.** (a) Initial constant-geometry FFT. (b) Pipelined constant geometry FFT. (c) Pipelined FFT based on cyclic rotations. (d) Pipelined phase-rotation FFT.

$$\begin{array}{ccc}
\begin{bmatrix} 0 & 2 & 4 & 6 \\ 1 & 3 & 5 & 7 \end{bmatrix} & \xrightarrow{\mathbf{S}} & \begin{bmatrix} 0 & 1 & 2 & 3 \\ 4 & 5 & 6 & 7 \end{bmatrix} \\
| \mathbf{C}_{slow} & & | \mathbf{C}_{fast} \\
\begin{bmatrix} 0 & 2 & 5 & 7 \\ 1 & 3 & 4 & 6 \end{bmatrix} & \xrightarrow{\bar{\mathbf{S}}} & \begin{bmatrix} 0 & 5 & 2 & 7 \\ 4 & 1 & 6 & 3 \end{bmatrix}
\end{array}$$

Figure 2: Replacing the perfect shuffle with three simpler shuffles.

We would like to replace the troublesome perfect shuffle operation with a *parallel-pipeline shuffle*, where each stream is read and written independently and in parallel. The next section describes the insights that make this possible.

### 2.3. The phase-rotation concept

This section describes how to replace the perfect shuffle by a parallel-pipeline shuffle, so that we can access the data streams in parallel. The basic idea is to rotate the data within frames, and then compensate for these motions by phase rotations of the twiddle factors.

We begin with a “detour” around the perfect shuffle. That is, we find a sequence of three simpler shuffles that is equivalent to the perfect shuffle. This idea is shown graphically in Figure 2 for an  $N$ -point radix-2 example. Each radix-2 pipeline segment is represented as matrix. Each row in the matrix corresponds to a stream, and each column corresponds to a frame. Frames (columns) are arranged left-to-right in reverse-time order in the matrix.

The first step in Figure 2 is a set of cyclic rotations, called  $\mathbf{C}_{slow}$ , which rotates each frame. These rotations are frame-wise in the sense that only data points contained in the same frame are rotated across the streams. Notice that in the radix-2 case, half of the rotations leave the corresponding frame unchanged. The next step is a parallel-pipeline shuffle  $\bar{\mathbf{S}}$ , which permutes the data in each stream. Notice that no data points need to be transferred between streams in this step. The last step is another set of frame-wise cyclic rotations, called  $\mathbf{C}_{fast}$ , which leave the data in the same order that the perfect shuffle would. Note that  $\mathbf{C}_{slow}$  and  $\mathbf{C}_{fast}$  change the number of rotations per frame at different paces, one slow and one fast. These varying rates are difficult to see in the radix-2 case, but are much more apparent in the higher-radix cases.

If we apply the idea in Figure 2) to each stage of the pipelined FFT in Figure 1(b), replacing each perfect shuffle with three simpler shuffles, we get a pipelined FFT based on cyclic rotations, which is shown in Figure 1(c).

The kind of basic frame-wise rotations in Figure 1(c) that is applied at slow-varying, and then fast-varying rates, is represented in general by the  $r \times r$  cyclic (circular) shift permutation matrix  $\mathbf{C}_r$ , made by permuting the rows of the identity matrix down by one row, and moving the bottom row up to the top. For

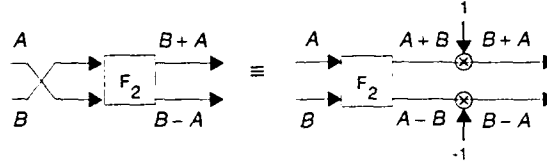


Figure 3: Interpretation of  $F_r C_r = D_r F_r$

example,

$$C_4 = \begin{pmatrix} 0 & 0 & 0 & 1 \\ 1 & 0 & 0 & 0 \\ 0 & 1 & 0 & 0 \\ 0 & 0 & 1 & 0 \end{pmatrix}.$$

The key insight of the phase-rotation FFT is that the cyclic shift theorem for the DFT can be applied to the cyclic shift operators in Figure 1(c). In matrix form, the cyclic shift theorem for a DFT is the relation

$$F_r C_r = D_r F_r, \quad (1)$$

where  $D_r = \text{diag}(1, \omega, \omega^2, \dots, \omega^{r-1})$  is a set of twiddles, and the DFT matrix of size  $r$  is

$$F_r = \frac{1}{\sqrt{r}} (\omega^{jk})_{j,k=0}^{r-1},$$

where  $\omega = e^{-\frac{2\pi i}{r}}$ . For the pipelined FFT, (1) says that phasor multipliers after a DFT kernel give the same effect as physical data rotations before the DFT kernel. Likewise, physical rotations after the kernel are equivalent to phasor multipliers before it. The meaning of (1) is shown graphically in Figure 3 for a pipelined radix-2 kernel. The shift theorem implies that the data rotations in Figure 1(c) can be replaced by constant phasor multipliers. These phasors can then be absorbed by the twiddle factors on either side of the kernel, leaving only a parallel-pipeline shuffle. The result is the pipelined phase-rotation FFT, which is shown in Figure 1(d). This completes the informal derivation of the phase-rotation FFT.

The structure of the phase-rotation FFT in Figure 1(d) is quite similar to the original pipelined FFT in Figure 1(b). The twiddle operators ( $D'$ ) are identical to the original twiddle operators ( $T$ ), except now the twiddles incorporate the original twiddles, phasor multipliers for the  $C_{fast}$  operator from the previous stage, and phasor multipliers for the  $C_{slow}$  operator from the next stage. The kernel operators are identical as well. The important difference is that the troublesome perfect shuffle operator has now been replaced by a parallel-pipeline shuffle that requires no communication across the streams.

There are several other important properties of the phase-rotation FFT. First, there are no additional multiplications or additions, compared to the original pipelined FFT in Figure 1(a). Second, the only internal communication across streams occurs at the kernel, and this communication is constrained, in that only data points within a single frame need to be switched across channels, and the switching is fixed for all frames.

### 3. Improved phase-rotation FFT

In this section we give a formal definition of an improved version of the original phase-rotation FFT described in [9]. The new version replaces the digit-reversing permutation in the original phase-rotation



FFT with a parallel-pipeline shuffle, followed by a frame-wise cyclic rotation. The advantage of this new approach is that during the digit-reversing step at the end, all communication between streams is limited to data points within a single frame.

For radix  $r$  and  $N = r^n$  points ( $n > 1$ ), the 1-dimensional phase-rotation FFT is a matrix factorization of the  $N$ -point DFT matrix  $F_N$ . Starting with the Pease constant-geometry factorization, we replace its perfect shuffles  $S$  by  $S = C_{fast} \bar{S} C_{slow}$ . Similarly, at the left end we replace the radix- $r$  index-digit-reversing permutation  $Q = Q_{N,r}$  of  $N$  data points by  $Q = C_{slow}^T \bar{Q} C_{slow}$ , where  $\bar{Q}$  is another parallel-pipeline shuffle that will be defined formally in Section 4. The phase-rotation FFT is then defined by:

$$\begin{aligned} F_N &= Q \cdot \prod_{j=1}^n (FST_j) = \cdots \left( \begin{array}{c} \text{vigorous} \\ \text{algebraic} \\ \text{shuffling} \end{array} \right) \cdots \\ &= C_{slow}^T \cdot \bar{Q} D'_{fast} \left[ \prod_{j=1}^n (F \bar{S} D'_j) \right] \cdot C_{slow}. \end{aligned} \quad (2)$$

Let  $s = N/r$  as before, and  $r' = N/r^2$ .  $F$  is a direct (tensor, Kronecker) product  $I_s \otimes F_r = \text{diag}(F_r, F_r, \dots, F_r)$ . We interpret this as a kernel DFT  $F_r$  operating on  $s$  successive frames of  $r$  points placed in the pipeline. For  $j = 1 : n$ , the other parts of (2) are defined by

$$\begin{aligned} C_{slow} &= \bigoplus_{k=0}^{r-1} (I_{r'} \otimes C_r^k) \\ C_{fast} &= I_{r'} \otimes \left( \bigoplus_{k=0}^{r-1} (C_r^T)^k \right) \\ \omega_j &= \exp\left(-\frac{2\pi i}{r^j}\right) \\ D_r &= \text{diag}(1, \omega_1, \omega_1^2, \dots, \omega_1^{r-1}) \\ D_{r^{j+1}} &= \text{diag}(1, \omega_{j+1}, \omega_{j+1}^2, \dots, \omega_{j+1}^{r^j-1}) \\ D_{slow}^{-1} &= \bigoplus_{k=0}^{r-1} (I_{r'} \otimes D_r^{-k}) \\ D'_{slow} &= C_{fast}^T D_{slow}^{-1} C_{fast} \\ D''_{slow} &= \bar{S}^T D'_{slow} \bar{S} \\ D_{fast}^{-1} &= I_{r'} \otimes \left( \bigoplus_{k=0}^{r-1} D_r^{-k} \right) \\ D'_{fast} &= C_{slow}^T D_{fast}^{-1} C_{slow} \\ \tilde{T}_j &= I_{\frac{N}{r^{j+1}}} \otimes \left( \bigoplus_{k=0}^{r-1} D_{r^{j+1}}^k \right) \\ T_j &= S^j T \tilde{T}_j S^j \\ T'_j &= C_{slow} T_j C_{slow}^T \\ D'_1 &= (\bar{S}^T D_{slow}^{-1} \bar{S}) \cdot T'_1 D_{fast}^{-1} \\ D'_j &= D''_{slow} T'_j D_{fast}^{-1} \quad j = 2 : n-1 \end{aligned}$$

$$\mathbf{D}'_n = \mathbf{D}''_{slow} \mathbf{T}'_n = \mathbf{D}''_{slow} \quad (3)$$

The direct sums are of the form

$$\bigoplus_{k=0}^{r-1} \mathbf{A}_k = \text{diag}(\mathbf{A}_0, \mathbf{A}_1, \dots, \mathbf{A}_{r-1}),$$

and  $\mathbf{A}^T$  denotes the transpose of  $\mathbf{A}$ . See [10] for more on the basic definitions and relations used to derive (2), as well as the generalization to higher dimension FFT's.

Note that the stages in (2) are counted in reverse time order by the index  $j$ . This is in keeping with the fact that (2) is a decimation-in-frequency (DIF) version of the FFT. The transpose of (2), with the product  $\prod_{j=n}^1$ , is the decimation-in-time (DIT) version of the phase-rotation FFT.

A  $\mathbf{C}_{slow}$  shuffle and its inverse remain at the input and output ends of the pipeline, respectively. As we have seen,  $\mathbf{C}_{slow}$  is a completely frame-wise rotation. It rotates (commutes) the data within each successive frame (column  $r$ -vector) of the  $r \times s$  pipeline segment for a stage. There is also an implicit frame-wise broadcast within each FFT kernel engine, when an  $r$ -point DFT is somehow computed. So in the phase-rotation FFT, data motion is all parallel, except for frame-wise motions at I/O and at every FFT kernel. The simplicity of the phase-rotation FFT is that no data point ever moves both down and across the pipeline in one time-step.

#### 4. Pipeline recipes

While the structure of the pipelined phase-rotation FFT is extremely simple, experience has taught us that generating the appropriate twiddles and shuffle indices from the matrix formulations of (2) and (3) is difficult and confusing. To address this problem, we have developed a collection of recipes for generating the phase-rotation twiddles and shuffle indices off-line. The recipes are defined for any 1D phase-rotation FFT of  $N = r^n$  points. Following [8], they are written in a MATLAB-like format.

As we saw in (2), the pipelined phase-rotation FFT performs a typical "twiddle, shuffle, kernel" cycle at each stage. Only the twiddles vary from stage to stage, and there is a digit-reversing shuffle equivalent at the end. To implement this FFT using parallel  $r \times s$  pipeline segments (one per stage), we insert the  $N$ -vector of input data  $\mathbf{x}$  into the pipeline as an  $r \times s$  array  $X$ : the first  $r$  points of  $\mathbf{x}$  go into the first frame (column)  $X$ , the second  $r$  points go into the second frame, and so on. We must also have a shuffle address and a twiddle factor ready for each point in the pipeline. In other words, we would like to fill one  $r \times s$  copy  $A$  of the pipeline segment with addresses, and another copy  $D$  with twiddles.

Then the processors in each stage of the pipeline will know what to do at each time-step  $t = 0:s-1$ . Using the current frame of addresses, they will fetch the current  $r$ -frame of data  $X(0:r-1, A(0:r-1, t))$  and the current  $r$ -frame of twiddles  $D(0:r-1, A(0:r-1, t))$  (pointwise in parallel), multiply these two frames pointwise, then do an  $r$ -point DFT  $\mathbf{F}_r$  of the twiddled data frame. That is how each stage  $\mathbf{FSD}'_j$  is implemented in the parallel pipeline.

The twiddle and shuffle recipes in this section are "in place" in the sense that they work inside the  $r \times s$  pipeline segments that will contain the desired addresses and twiddles. They are not "in place" in the usual sense, as we will freely use an input and an output copy of a pipeline segment. This approach avoids constructing and operating with large  $N \times N$  matrices (each containing only  $N$  non-zero elements). Each

parallel-pipeline function recipe is given a name similar to that of the  $N \times N$  matrix factor in the FFT (2) that it effectively implements.

#### 4.1. Shuffle recipes

As a convention, pipeline addresses (pipeline array row and column indices) run  $0:r-1$  and  $0:s-1$ , respectively. To do parallel-pipeline shuffles, we only need the horizontal (column) addresses, since the data inside each pipe will only jump within that stream (row). The cross-stream shuffles, Cslow and Cfast, are implemented using  $\pi_r$ , a cyclic rotation of a frame (a vertical slice of the parallel pipeline) that has the effect of  $\mathbf{y}_r = \mathbf{C}_r \mathbf{x}_r$ .  $\pi_r$  takes a column  $r$ -vector  $\mathbf{x}_r = (x_0, x_1, x_2, \dots, x_{r-1})^T \mapsto \mathbf{y}_r = (x_{r-1}, x_0, x_1, \dots, x_{r-2})^T$ .

```

function Y = Cslow(X)
col = 0
for k = 1 : r
    for j = 1 : r'
        Y(:, col) =  $\pi_r^k(X(:, col))$ 
        col = col + 1
    end
end

```

```

function Y = Cfast(X)
col = 0
for j = 1 : r
    for k = 1 : r'
        Y(:, col) =  $\pi_r^k(X(:, col))$ 
        col = col + 1
    end
end

```

The inverses of Cslow and Cfast are formed by simply reversing  $\pi_r$ . Next, we define some perfect shuffles.

```

function Y = S(X) %!stride by s
col = 0
for row = 0 : r - 1
    for k1 = 0 : r : s - r
        k2 = k1 + r - 1
        Y(row, k1 : k2) = X(:, col)
        col = col + 1
    end
end

```

```

function Y = S-1(X) %!stride by r
col = 0
for row = 0 : r - 1

```

```

    for  $k1 = 0 : r : s - r$ 
         $k2 = k1 + r - 1$ 
         $Y(:, col) = X(row, k1 : k2)$ 
         $col = col + 1$ 
    end
end

```

To implement the parallel-pipeline shuffles,  $\bar{\bar{S}}$ ,  $\bar{\bar{S}}^{-1}$ , and  $\bar{\bar{Q}}$ , we will use the parallel-pipeline addresses  $A$ , which are computed by the following function:

```

function  $A = \bar{\bar{S}}\_addresses(r, s)$ 
 $a = (0, r', \dots, (r - 1)r')^T$ 
 $col = 0$ 
for  $j = 1 : r'$ 
    for  $k = 1 : r$ 
         $A(:, col) = a$ 
         $col = col + 1$ 
         $a = \pi_r(a)$ 
    end
     $a = a + 1_r$ 
end

```

Looking closely, one can see  $Cfast^{-1}$  at work producing the addresses  $A$  in the last function. The addresses  $A$  can also be generated by loading a pipeline segment with simple  $r \times r$  address blocks  $B_{rr}$ , and then applying  $Cfast^{-1}$  to the pipeline segment. The first block to load is  $B_{rr} = \text{diag}(0:r':s-1) * 1_{rr}$ , where  $1_{rr}$  is the  $r \times r$  matrix whose entries are all 1's. The next block is always  $B_{rr} = B_{rr} + 1_{rr}$ , until the pipeline segment contains  $r'$  blocks and is full.

```

function  $Y = \bar{\bar{S}}(X)$ 
 $A = \bar{\bar{S}}\_addresses(r, s)$ 
for  $row = 0 : r - 1$ 
     $Y(row, :) = X(row, A(row, :))$ 
end

```

```

function  $Y = \bar{\bar{S}}^{-1}(X)$ 
 $A = \bar{\bar{S}}\_addresses(r, s)$ 
 $[AA, I] = \text{sort}(A)$ 
for  $row = 0 : r - 1$ 
     $Y(row, :) = X(row, I(row, :))$ 
end

```

In the above functions,  $\text{sort}(A)$  sorts each row of an array  $A$  in ascending order. It returns the row-sorted array  $AA$  and the corresponding array of addresses  $I$  where the successive row elements were found in  $A$ . After we have sorted the addresses  $A$  for  $\bar{\bar{S}}$ ,  $I$  has the addresses for  $\bar{\bar{S}}^{-1}$ .

The pipeline addresses for  $\bar{\bar{Q}}$  are obtained by block-perfect shuffles (along the length of the pipeline) of the addresses for  $\bar{S}$ :

```
function Y =  $\bar{\bar{Q}}$ (X, n)
A =  $\bar{S}$ _addresses(r, s)

if n > 2
    for ns = (n - 2) : -1 : 1
        stride =  $r^n s$ 
        block =  $r^{n-2-ns}$  ! block length
        col2 = 0
        for k1 = 1 : stride
            col1 = (k1 - 1) * block
            for k = 1 : r
                for j = 1 : block
                    B(:, col2) = A(:, col1)
                    col1 = col1 + 1
                    col2 = col2 + 1
                end
                col1 = col1 + (stride - 1) * block
            end
        end
        A = B
    end
end

for row = 0 : r - 1
    Y(row, :) = X(row, A(row, :))
end
```

#### 4.2. Twiddle recipes

Every twiddle matrix  $D$  is diagonal, so it operates on a data vector as a point-to-point vector multiply. Given some permutation matrix  $P$ , a new twiddle matrix  $PDP^T$  is equivalent to a re-diagonalizing of the vector shuffle of the diagonal of  $D$ , that is,  $PDP^T = \text{diag}(P * \text{diag}(D))$ . (This is a MATLAB notation:  $\text{diag}()$  puts the diagonal of a matrix in a vector, and puts a vector in the diagonal of a matrix.) Since we want to perform shuffles within pipeline arrays, we reshape the twiddle  $N$ -vector  $\text{diag}(D)$  as an  $r \times s$  pipeline array  $D$ , just as we originally reshaped the data vector. Then we shuffle the pipelined twiddles, to effect the equivalent of the vector shuffle- $P * \text{diag}(D)$ . So we interpret the  $PDP^T$  operator as an in-pipeline shuffle of the pipelined twiddles  $D$ , which are then in position to operate on the pipelined data  $X$  directly by point-to-point multiplication,  $Y = D * X$ . (As mentioned, the data will actually be twiddled frame-by-frame in the pipelined implementation.)

We will interpret the twiddles expressed in (3) this way. Each twiddle function below returns an  $r \times s$  array  $D$  of twiddle factors (the actual twiddling of the data is not included):

```

function  $D_{slow} = D_{slow\_twiddles}(r, s)$ 
 $\omega_j = \exp(-2\pi i/r)$ 
 $t = 0$ 
for  $j = 0 : (r - 1)$ 
  for  $k = 0 : (r' - 1)$ 
     $D_{slow}(:, t) = (1, \omega_r^k, \omega_r^{2k}, \dots, \omega_r^{(r-1)k})^T$ 
     $t = t + 1$ 
  end
end

```

```

function  $D_{fast} = D_{fast\_twiddles}(r, s)$ 
 $\omega_j = \exp(-2\pi i/r)$ 
 $t = 0$ 
for  $k = 0 : (r' - 1)$ 
  for  $j = 0 : (r - 1)$ 
     $D_{fast}(:, t) = (1, \omega_r^j, \omega_r^{2j}, \dots, \omega_r^{(r-1)j})^T$ 
     $t = t + 1$ 
  end
end

```

The inverses of  $D_{slow}$  and  $D_{fast}$  are just their complex conjugates, and are generated simply by replacing  $\omega_j$  by  $\omega_j^{-1}$ . For stages  $j = 1:n$  (counted down from  $n$ ), we generate pipelined twiddles  $\tilde{T}_j$  by

```

function  $\tilde{T}_j = \tilde{T\_twiddles}(r, s, j)$ 
 $\omega_j = \exp(2\pi i/r^{j+1})$ 
 $\omega'_j = \omega_{r^{j+1}}^*$ 
for  $k = 0 : (r - 1)$  ! direct sum loop
   $t_1 = k \cdot r^{j-1}$ 
  for  $p = 0 : (r - 1)$ 
     $\tilde{T}_j(p, t_1) = \omega_j^{kp}$ 
  end
   $t_1 = t_1 + 1$ 
   $t_2 = t_1 + r^{j-1}$ 
  for  $t = t_1 : t_2$  ! fill next column from last
     $\tilde{T}_j(:, t) = \omega_j'^k \cdot \tilde{T}_j(:, t - 1)$ 
  end
end

if  $j < n$ 
   $t_2 = r^j$ 
  for  $k = 0 : (N/r^{j+1})$ 
     $t_1 = t_2$ 
     $t_2 = k \cdot r^j$ 
     $t = 0$ 
    for  $t_0 = t_1 : t_2$ 

```

```

         $\hat{T}_j(:, t_0) = \hat{T}_j(:, t) \quad \text{! copy columns}$ 
         $t = t + 1$ 
    end
end
end

```

The rest of the twiddle arrays can now be defined in terms of the shuffles:

```

 $D'_{slow} = S^{-1}(D_{slow}^{-1})$ 
 $D''_{slow} = \text{Cslow}(D'_{slow})$ 

 $D'_{fast} = \text{Cslow}(D_{fast}^{-1})$ 

 $T_j = S^{-1}(\hat{T}_j)$ 
 $T'_j = \text{Cslow}(T_j)$ 

 $D'_1 = \bar{S}(D_{slow}^{-1}) * T'_1 * D_{fast}^{-1}$ 
if  $1 < j < n$ 
     $D'_j = D''_{slow} * T'_j * D_{fast}^{-1}$ 
end
 $D'_n = D''_{slow}$ 

```

## 5. Implementation issues

In this section we describe issues that arise when the phase-rotation FFT is implemented on a real parallel system. In particular, we describe implementation approaches for the radix-2 FFT on the iWarp system. The main result is a scalable implementation of the pipelined phase-rotation FFT that runs at the full 40 Mbytes/second rate of the iWarp physical links.

### 5.1. iWarp

The iWarp is a private-memory multicomputer developed jointly by Intel and Carnegie Mellon [1, 2]. iWarp systems are 2-dimensional tori of iWarp nodes, ranging in size from 4 to 1024 nodes. Each node consists of an iWarp component, up to 16 Mbytes of off-chip local memory, and a set of 8 unidirectional communication links that physically connect the node to four neighboring nodes.

The iWarp component is a VLSI chip that contains a *processing agent* and a *communication agent*. The processing agent is a general-purpose load-store microprocessor, centered around a  $128 \times 32$ -bit register file, that runs at a maximum rate of 20 MFLOPs. The local memory is accessed at a rate of 160 Mbytes/sec. Each link runs at 40 Mbytes/sec, for a maximum aggregate bandwidth of 320 Mbytes/sec per node.

The key feature of the iWarp is its communication system, which is summarized in Figure 4. Each communication agent contains a set of 20 hardware FIFO queues. Each queue can hold up to 8 32-bit words. iWarp nodes communicate with other nodes using unidirectional point-to-point structures called

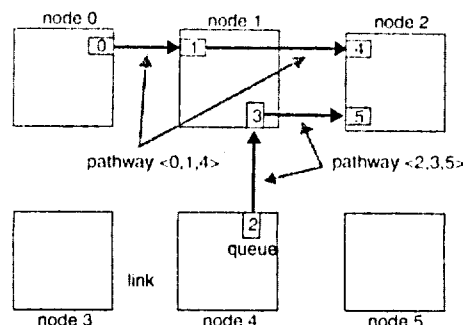


Figure 4: iWarp communication concepts.

pathways. Each pathway is a sequence of queues. Pathways can be created and destroyed dynamically at runtime. Figure 4 shows a pair of such pathways.

Data traveling along a pathway passes from queue to queue *automatically*, without disturbing the computations on intermediate nodes. For example, in Figure 4, data items traveling over the pair of pathways do not disturb the computation on node 1. The latency from queue to queue is small, ranging from 100-300 nanoseconds.

Multiple pathways can share the same link. For example, in Figure 4, two pathways share the link from node 1 to node 2. In this case, the pathways share the link bandwidth in a round-robin fashion, one word at a time. If only one pathway is sending data over a link, then it gets the entire link bandwidth. If multiple pathways are sending data over a link, then the link can be utilized at the full 40 Mbytes/sec, and each pathway is guaranteed a proportional fraction of the bandwidth.

User programs can directly access the queues, one word at a time, by reading and writing special registers in the register file called *gates*. To an iWarp instruction, a gate is just another register in the register file. The important point is that a program can read or write a word in a queue with the latency of a register access. A single instruction can read and write up to 4 words from queues, with a maximum aggregate bandwidth of 160 Mbytes/sec. Gates can be accessed directly from user-level C programs.

## 5.2. Mapping strategies on iWarp

The problem is to develop a mapping of the flowgraph in Figure 1(d) to an iWarp array. The simplest mapping strategy is to assign each flowgraph node to a unique processor node of a linear array, route the flowgraph arcs through this array, and then embed the resulting linear array in the iWarp torus. This approach, called the PHASE5 mapping because it uses 5 iWarp nodes for each FFT stage, is shown in Figure 5(a).

Each iWarp node in PHASE5 executes a small *node program* that implements its flowgraph operator. Each twiddle node ( $D'$ ) repeatedly reads a complex number from its input pathway (via the gates), multiplies it by the appropriate twiddle (precomputed off-line using the recipes in Section 4.2), and sends the result to its output pathway (again, via the gates). Each shuffle operator ( $\bar{S}$ ) repeatedly reads a complex data item from its input pathway, stores it in memory, and uses the appropriate shuffle index (again precomputed off-line using the recipes in Section 4.1) to send an appropriate double-buffered data point to the output



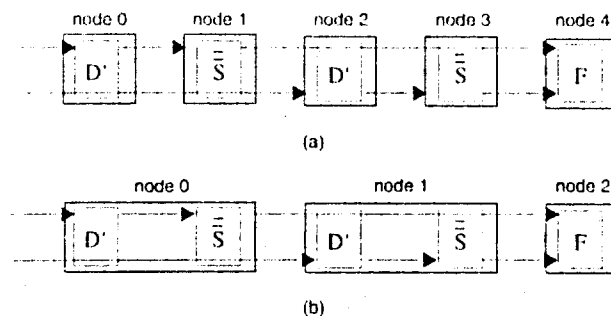


Figure 5: Strategies for mapping one stage of the FFT onto a linear array. (a) PHASE5 mapping. (b) PHASE3 mapping.

pathway. The kernel node ( $F$ ) repeatedly reads two complex numbers from its input pathways, performs the radix-2 DFT kernel operation, and outputs two complex numbers to its output pathways.

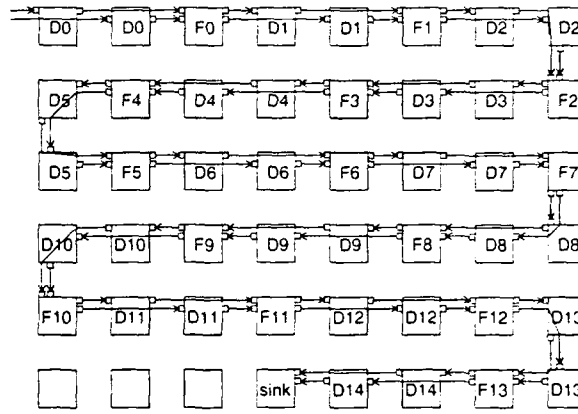
Another approach, the PHASE3 mapping, combines the twiddle and shuffle operators on a single node, as shown in Figure 5(b), so that each stage requires 3 nodes instead of 5 nodes. As we shall see, the communication and computation throughputs of the two mappings are identical. The advantage of the PHASE3 mapping is that it is more node-efficient, requiring fewer nodes per stage than the PHASE5 mapping. The advantage of the PHASE5 mapping is its simplicity. Each node is assigned exactly one operator from the flowgraph.

Figure 6 shows a working implementation of a 16K-point radix-2 phase-rotation FFT on a 64-node iWarp array at Carnegie Mellon. The large squares are iWarp nodes, labeled with the corresponding operator and stage number. The small squares are queues. The arrows are iWarp pathways. The implementation is based on the PHASE3 mapping from Figure 5(b). Each of the 14 FFT stages uses 3 nodes, with an additional 3 nodes for the parallel-pipeline digit-reversing step at the end.

### 5.3. Performance

While the details are beyond the scope of this paper, each iteration of each node program in the PHASE3 and PHASE5 mappings runs in at most 8 clocks. At the peak rate of 40 Mbytes/sec, each link can produce and consume a 32-bit floating-point number every 2 clocks. Further, each data point in the pipeline is a complex number consisting of a pair of 32-bit floating-point words. As a result, each pathway requires exactly half of the available link bandwidth. Since each link is shared by two pathways, and since the iWarp communication agent gives each pathway an equal share of the link bandwidth, without disturbing the computations on intermediate nodes, each link is fully utilized. The result is a radix-2 FFT that runs at the full 40 Mbytes/sec rate of an iWarp link, regardless of the number of points in the FFT! Since each sample consists of 8 bytes, the FFT runs at a constant rate of 5 Msamples/sec. Given a sufficient number of nodes, the iWarp phase-rotation FFT's will produce arbitrarily large FFT's at this rate. Perhaps even more important, the performance is the same on smaller FFT's.

Another way to characterize the performance of the PHASE3 and PHASE5 mappings is by its computational throughput, expressed as millions of floating-point operations per second (MFLOPS). However, there is a subtlety involved in using MFLOPS as a performance measure. The iWarp phase-rotation FFT



**Figure 6: 16K-point pipelined phase-rotation FFT running at 40 Mbytes/sec (350 MFLOPS) on iWarp**

performs performs 16 floating-point operations per iteration per stage (2 adds and 4 multiplies by each twiddle operator, and 4 adds by the kernel operator). But the standard formula for computing FFT MFLOPS is  $5N \log N$  floating-point operations per  $N$ -point FFT [3], which implies 10 floating-point operations per iteration per stage. Therefore, in order to do fair comparisons with other FFT algorithms, we must compute the phase rotation performance using the standard of 10 floating-point operations per iteration per stage, even though the phase-rotation FFT is actually performing 16 floating-point operations per iteration per stage.

Since each node program executes its computation in at most 8 clocks, and since each clock is 50 nanoseconds, each stage of the iWarp phase-rotation FFT runs at a rate of

$$\frac{10 \text{ fp operations}}{8 \text{ clocks}} \times \frac{1 \text{ clock}}{50 \text{ nanoseconds}} \times \frac{1 \times 10^9 \text{ nanoseconds}}{1 \text{ second}} = 25 \text{ MFLOPS}$$

for a total performance over all of the  $\log N$  stages of  $25 \log N$  MFLOPS. For example, the 16K-point FFT in Figure 6 achieves a measured performance of  $25 \times 14 = 350$  MFLOPS (single precision) on iWarp. As a point of comparison, a highly optimized 16K-point FFT has been measured at 237 MFLOPS (double precision) on a single-processor Cray Y-MP [3, p.114]. The numbers are not directly comparable because of the different floating-point precisions, but they do suggest that the absolute performance of the phase-rotation FFT on iWarp is quite good.

## 6. Concluding remarks

We have described an improved version of the Whelchel pipelined phase-rotation FFT, developed recipes for generating the appropriate twiddles and shuffle indices off-line and directly in terms of the parallel pipeline, outlined mapping approaches for the radix-2 case on pthe iWarp parallel computer, and presented measured performance results of an implementation on iWarp.

The improvement on the original phase-rotation FFT is significant in that it eliminates a potential pipeline bottleneck during the digit reversing step at the end. The twiddle and shuffle recipes should be helpful

to the programmer who wants to implement the pipelined phase rotation FFT. The iWarp implementation validates a simple and realistic approach for building scalable pipelined FFT's on a programmable parallel system. Further, the implementation demonstrates that, given a balanced parallel computer architecture with word-level access to the communication links, it is possible to build FFT's that run at the full link bandwidth of the links, even when the FFT's are relatively small.

## Acknowledgements

We would like to thank Tom Warfel and LeeAnn Tzeng for their help with the iWarp implementation, and Doug Noll and Doug Smith for discussions that led to the more node-efficient mapping.

## References

- [1] BORKAR, S., COHN, R., COX, G., GLEASON, S., GROSS, T., KUNG, H. T., LAM, M., MOORE, B., PETERSON, C., PIEPER, J., RANKIN, L., TSENG, P. S., SUTTON, J., URBANSKI, J., AND WEBB, J. iWarp: An integrated solution to high-speed parallel computing. In *Supercomputing '88* (Nov. 1988), pp. 330-339.
- [2] BORKAR, S., COHN, R., COX, G., GROSS, T., KUNG, H. T., LAM, M., LEVINE, M., MOORE, B., MOORE, W., PETERSON, C., SUSMAN, J., SUTTON, J., URBANSKI, J., AND WEBB, J. Supporting systolic and memory communication in iWarp. In *Proceedings of the 17th Annual International Symposium on Computer Architecture* (Seattle, WA, May 1990), pp. 70-81.
- [3] CARLSON, D. Ultra-performance FFTs for the CRAY-2 and CRAY Y-MP supercomputers. *Journal of Supercomputing* 6 (1992), 107-115.
- [4] COOLEY, J., AND TUKEY, J. An algorithm for the machine computation of complex Fourier series. *Mathematics of Computation* 19 (Apr. 1965), 297-301.
- [5] CORINTHIOS, M. The design of a class of Fast Fourier Transform computers. *IEEE Transactions on Computers* C-20 (June 1971), 617-623.
- [6] MCCLELLAN, J., AND PURDY, R. Radar signal processing. In *Applications of Digital Signal Processing*, A. Oppenheim, Ed. Prentice-Hall, Englewood Cliffs, NJ, 1978.
- [7] PEASE, M. An adaptation of the Fast Fourier Transform for parallel processing. *Journal of the Association for Computing Machinery* 15 (1968), 252-264.
- [8] VAN LOAN, C. *Computational Frameworks for the Fast Fourier Transform*. SIAM, Philadelphia, PA, 1992.
- [9] WHELCHER, J., O'MALLEY, J., RINARD, W., AND MCARTHUR, J. The systolic phase rotation FFT - a new algorithm and parallel processor architecture. In *Proceedings of ICASSP '90* (Apr. 1990), pp. 1021-1024.
- [10] WITHERS, JR., L., AND WHELCHER, J. The multidimensional phase-rotation FFT - a new parallel architecture. In *Proceedings of ICASSP '91* (May 1991), pp. 2889-2892.

# REPORT DOCUMENTATION PAGE

Form Approved  
OMB No. 0704-0188

Public reporting burden for this collection of information is estimated to average 1 hour per response, including the time for reviewing instructions, searching existing data sources, gathering and maintaining the data needed, and completing and reviewing the collection of information. Send comments regarding this burden estimate or any other aspect of this collection of information, including suggestions for reducing this burden, to Washington Headquarters Services, Directorate for Information Operations and Reports, 1215 Jefferson Davis Highway, Suite 1204, Arlington, VA 22202-4302, and to the Office of Management and Budget, Paperwork Reduction Project (0704-0188), Washington, DC 20503.

1. AGENCY USE ONLY (Leave blank)		2. REPORT DATE		3. REPORT TYPE AND DATES COVERED	
4. TITLE AND SUBTITLE Computing the Pipelined Phase-Rotation FFT				5. FUNDING NUMBERS	
6. AUTHOR(S) Langhorne P. Withers, Jr., John E. Whelchel, David R. O'Hallaron, Peter J. Lieu					
7. PERFORMING ORGANIZATION NAME(S) AND ADDRESS(ES) School of Computer Science Carnegie Mellon University Pittsburgh, PA 15213-3891				8. PERFORMING ORGANIZATION REPORT NUMBER CMU-CS-93-174	
9. SPONSORING/MONITORING AGENCY NAME(S) AND ADDRESS(ES) ARPA/CMO AFOSR				10. SPONSORING/MONITORING AGENCY REPORT NUMBER MDA972-90-C-0035 F49620-92-J-0131	
11. SUPPLEMENTARY NOTES					
12a. DISTRIBUTION/AVAILABILITY STATEMENT Unlimited distribution				12b. DISTRIBUTION CODE (A)	
13. ABSTRACT (Maximum 200 words) See titlepage.					
14. SUBJECT TERMS See reverse of titlepage				15. NUMBER OF PAGES 16	
				16. PRICE CODE	
17. SECURITY CLASSIFICATION OF REPORT	18. SECURITY CLASSIFICATION OF THIS PAGE	19. SECURITY CLASSIFICATION OF ABSTRACT	20. LIMITATION OF ABSTRACT		

---

School of Computer Science  
Carnegie Mellon University  
Pittsburgh, PA 15213-3890

Carnegie Mellon University does not discriminate and Carnegie Mellon University is required not to discriminate in admission, employment or administration of its programs on the basis of race, color, national origin, sex or handicap in violation of Title VI of the Civil Rights Act of 1964, Title IX of the Educational Amendments of 1972 and Section 504 of the Rehabilitation Act of 1973 or other federal, state or local laws, or executive orders.

In addition, Carnegie Mellon University does not discriminate in admission, employment or administration of its programs on the basis of religion, ~~creed~~, ancestry, belief, age, veteran status, ~~sexual orientation~~ or violation of federal, state or local laws, or executive orders.

Inquiries concerning application of these statements should be directed to the Provost, Carnegie Mellon University, 5000 Forbes Avenue, Pittsburgh, PA 15213, telephone (412) 268-6684 or the Vice President for Enrollment, Carnegie Mellon University, 5000 Forbes Avenue, Pittsburgh, PA 15213, telephone (412) 268-2056.

---